Pergamon

Journal of Atmospheric and Terrestrial Physics, Vol. 58, No. 6, pp. 661–672, 1996
Copyright © 1996 Elsevier Science Ltd
Printed in Great Britain. All rights reserved
0021–9169/96 $15.00+0.00

0021-9169(95)00065-8

Further effects of charged aerosols on summer mesospheric radar scatter

John Y. N. Cho,* Christian M. Alcala,† Michael C. Kelley† and Wesley E. Swartz†

*Arecibo Observatory, P.O. Box 995, Arecibo, Puerto Rico 00613 †School of Electrical Engineering, Cornell University, Ithaca, New York 14853, USA

(*Received in final form* 1 *November* 1994; *accepted* 23 *November* 1994)

Abstract—In an earlier paper, we showed that charged aerosols play a crucial role in enhancing radar echoes from the summer polar mesosphere through reduced diffusion turbulent scatter and dressed aerosol scatter (Cho *et al.*, 1992a). Here, we explore the effects of charged aerosols on radar scatter through 'fossil' turbulence and electron density depletion layers. We find that the former can produce radar scatter even after the decay of neutral gas turbulence, while the latter, which are probably produced by the scavenging of free electrons by ice particles, are a candidate for causing partial reflection or Fresnel scatter. Furthermore, we examine the mutual aerosol interaction restriction on dressed aerosol scatter more closely. We find that a high ambient electron density and low aerosol number density are needed for effective dressed aerosol scatter to occur. We then show that very small (less than 1 nm radii), negatively charged aerosols enhance electron diffusivity, and thus inhibit radar scatter. Also, ice aerosol sedimentation, in the light of the reduced diffusion theory, leads us to conclude that the statistical peak in Polar Mesospheric Summer Echoes (PMSE) power should be located between the mean mesopause and the average noctilucent cloud (NLC) height, which agrees with observations. Finally, we invoke time lags in the ice particle formation cycle to account for the observed non-correlation between PMSE and NLC occurrence.

1. INTRODUCTION

The Earth's atmosphere in the mesopause region is weakly ionized and dusty, due to its location at the bottom of the ionosphere and in the meteor ablation zone. Furthermore, in the summer (especially in the polar region) its temperatures are the lowest in the atmosphere, which is believed to be the result of adiabatic cooling driven by a filtered gravity wave mechanism originating in the lower atmosphere. The presence of nucleation sites, such as meteoric dust, then leads to the formation of ice particles which, when grown large enough, appear visibly as noctilucent clouds, the highest clouds on Earth. Thus, the summer mesopause atmosphere can be characterized succinctly as a weakly ionized dusty ice plasma, a product of complex coupling processes from above and below.

Ecklund and Balsley (1981) discovered that a 50 MHz radar received an enormous amount of backscatter from the summer polar mesopause. A similar effect was observed at 224 MHz (Hoppe *et al.*, 1988), and weaker enhancements were seen at 933 MHz (Röttger *et al.*, 1990) and 1290 MHz (Cho *et al.*, 1992b). Röttger *et al.* (1988) introduced the acronym PMSE (polar mesosphere summer echoes) to describe this phenomenon. For further details, we refer the reader to our recent review of PMSE (Cho and Kelley, 1993).

Building on the ideas of Kelley *et al.* (1987), Cho *et al.* (1992a) showed that the presence of electrically charged aerosols in the mesosphere leads to enhancement in the radar Bragg scatter. Here, we briefly summarize the results. Mesospheric radar scatter is caused by inhomogeneities in the plasma electron density. Outside of the summer mesopause region, fluctuations in the electron density are rapidly smoothed by diffusion and thus the radar scattering is weak. However, in the cloudy summer mesopause region the electrons become electrically coupled to the large, slowly diffusing, charged ice aerosols; the consequent reduction of electron diffusivity results in the maintenance of electron inhomogeneities at the radar Bragg scales. This theory links the presence of ice particles with enhanced radar scatter regardless of the mechanism that created the electron fluctuations in the first place; therefore, it explains the high degree of correlation between a cold mesopause and strong radar echoes. Applied to a particular fluctuation producer, neutral turbulence, the theory was able to produce reasonably the highest reflectivities observed at

50 and 224 MHz. Comparisons with rocket measurements of electron density fluctuations also showed instances in which the radar reflectivity predicted by reduced-diffusion turbulent scatter (or equivalently, raised Schmidt number scatter) agreed well with the observed radar echoes (Kelley and Ulwick, 1988; Kelley *et al.*, 1990). Recently, Klostermeyer (1994) applied a height-dependent two-ion-plus-ice-particle model to the reduced-diffusion turbulent scatter mechanism that yielded reasonable results at VHF.

For the PMSE observed at the higher radar frequencies, the above theory required very large, highly charged aerosols, the existence of which is debatable. The upper limit in size, for example, is set by the visible cloud particles that occur only sporadically. In turn, the charge per aerosol is generally believed to be limited by this size and the temperature of the ambient electrons if photoemission is ignored. The result is that, even the largest ice aerosol should not be charged more than by ~ -4 elementary charges. However, this is somewhat controversial since very little is known about the true composition of the aerosols. A dressed aerosol effect proposed by Havnes *et al.* (1990) was investigated as an alternative, but this theory also requires highly charged aerosols. Clearly, more work is needed to understand PMSE in the UHF regime.

Furthermore, there is more and more evidence that PMSEs occur in both turbulent and laminar contexts with characteristics, in the latter case, of Fresnel scatter or partial reflection, i.e. aspect sensitivity and narrow Doppler spectra. Figure 1 shows a case in which an upper PMSE layer is isotropic and the lower one is aspect sensitive. The Doppler spectra were narrower in the lower layer than in the upper one (Cho *et al.*, 1993). Rocket measurements made at the same time confirmed the presence of neutral and plasma turbulence in the upper layer and no neutral turbulence but edge-like plasma inhomogeneities in the lower layer (Lübken *et al.*, 1993; Ulwick *et al.*, 1993).

In this paper we will investigate the effects of charged aerosols on mesospheric radar scatter in situations where neutral gas turbulence is not the primary plasma fluctuation producer. We will also discuss the special case of very small, negatively charged aerosols. Finally, we will consider the effects of aerosol sedimentation and the time lags associated with the ice cloud formation cycle.

2. FOSSIL TURBULENCE

Imagine going to the bottom of a waterfall and releasing a tank of tracer dye where the pool is turbulent (see Fig. 2). Now run downstream to a section where the flow is laminar and wait for the initial release to reach you. Trickle in the dye again and note that it describes a fairly straight line. The original tracer, however, retains a turbulent look as it is carried past you by the current.

What has happened, of course, is that the turbulence-like spatial structures in the scalar additive (the dye), mixed by turbulence, has survived beyond the decay of turbulence itself. The term 'fossil turbulence' was coined by Woods (1969) to describe this phenomenon. Note that fossil turbulence is not turbulence, just as fossil trilobites are not trilobites—just their imprints. However, unlike fossil trilobites, fossil turbulence is not frozen in time; it begins with kinetic energies of the order of the original turbulence and decays with time. Much of the subject has revolved around oceanic observations of temperature fluctuations. (The reader is referred to Gibson, 1991 for a review.) We propose that fossil turbulence may be of relevance in PMSE. Because of the very slow diffusivity of the aerosols, some PMSE may result from a fossilized plasma even after the decay of the neutral gas turbulence that produced the density inhomogeneities.

The following scenario unfolds after the source of kinetic energy is removed from the turbulent mixing of a high Schmidt number scalar additive, where the Schmidt number is defined as $Sc = \nu D_\xi^{-1}$, with ν the fluid viscosity and D_ξ the scalar diffusivity (see Fig. 3). Begin with a turbulent patch of length scale L_p embedded in a non-turbulent, stably stratified region with an ambient vertical gradient in the scalar (curve labelled 'A'). With no energy input, the velocity fluctuation spectrum starts to decay and the inertial subrange shrinks as the Kolmogorov inner scale, $l_K = \nu^{3/4}\varepsilon^{-1/4}$ (Kolmogorov, 1941), moves to longer lengths; the size of the patch grows due to the entrainment of ambient fluid, and the Batchelor scale (Batchelor, 1959), $l_B = \nu^{1/4} D_\xi^{1/2} \varepsilon^{-1/4}$, where ε is the turbulence energy dissipation rate of the scalar variance spectrum, also shifts to larger scales, but the level of the spectrum rises because the difference in the scalar quantity between fluid entrained at the top and bottom increases as the patch grows (curve labelled 'B'). (l_B is essentially the cut-off scale where shorter length scale fluctuations are immediately destroyed by diffusion.)

Fossilization sets in as L_p grows to l_{LS}, the Lumley–Shur buoyancy scale (Shur, 1962; Lumley, 1964), defined by $l_{LS} = \omega_B^{-3/2}\varepsilon^{1/2}$ where ω_B is the Brunt–Väisälä frequency. (l_{LS} is the upper scale length limit for the existence of turbulence. In fossil turbulence literature, the buoyancy scale is often referred to as the Ozmidov scale.) At this point, the inertial forces

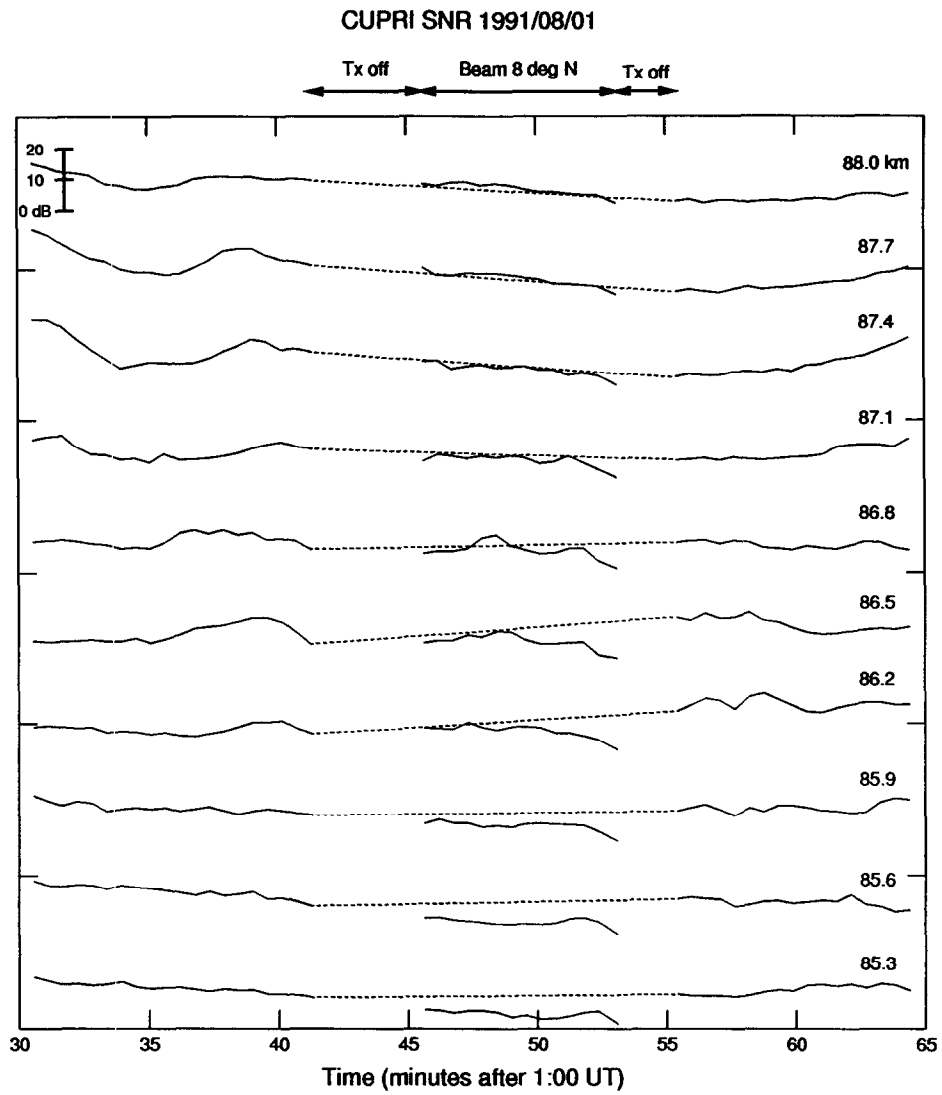

Fig. 1. Cornell University portable radar interferometer (CUPRI) signal-to-noise ratio (SNR) values are plotted for the height range where PMSE existed during Salvo B of the noctilucent cloud-91 (NLC-91) rocket and radar campaign conducted in Esrange, Sweden. In the central time slice of the plot, the radar beam was shifted from vertical to 8°N. The horizontally dashed lines simply connect the SNR value last observed before beam-swinging to the first value recorded after shifting back to vertical.

become approximately equal to the buoyancy forces. Complete fossilization is deemed to be reached when the viscous dissipation rate subsides to $\varepsilon = 24.5\nu\omega_B^2$ (Stillinger *et al.*, 1983) and the Batchelor scale has reached the fossil Batchelor scale $l_{BF} = D^{1/2}\omega_B^{-1/2}$ (Gibson, 1986) (curve labelled 'C'). The actual break-points occur at $C_B l_B$ and $C_B l_{BF}$ where $C_B \approx 4$ (Gibson, 1982).

Gibson (1980) gives a scalar fossil 'decay time' of $\tau_F = \varepsilon_0^{1/3}\nu^{-1/3}\omega_B^{-5/3}$ where ε_0 is the energy dissipation rate at the onset of fossilization, which lies between the ε of the original turbulence and $\varepsilon_F = 24.5\nu\omega_B^2$, which occurs at complete fossilization. ($\varepsilon_F \approx 8$ mW/kg^{-1} for the summer mesopause.) The time τ_F can be taken as the minimum persistence time of the scalar density variance, because after fossilization the ultimate dissipation is controlled by the scalar diffusion time, which depends on the diffusivity and length scale of the inhomogeneity. The diffusion time scale is $\tau_d = k^{-2}D_\xi^{-1}$ where k is the wave-number

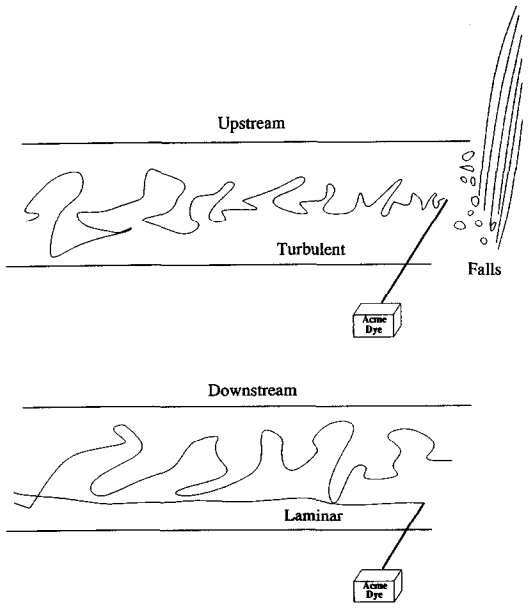

Fig. 2. Schematic of dye release *gedanken* experiment.

of the scalar density fluctuation. For k corresponding to a length scale of 3 m and D_ξ of an aerosol of radius 0.01 μm, we get $\tau_d \approx 4$ min (see Cho *et al.*, 1992a, for diffusivity formula). Turbulence dissipation energy $\varepsilon_0 \approx 10\ \text{mW/kg}^{-1}$ translates to $\tau_F \approx 3$ min. So we see that 3 m (50 MHz radar Bragg scale) density fluctuations of aerosols of size 0.01 μm will persist of the order of 7 min after the cessation of neutral gas turbulence.

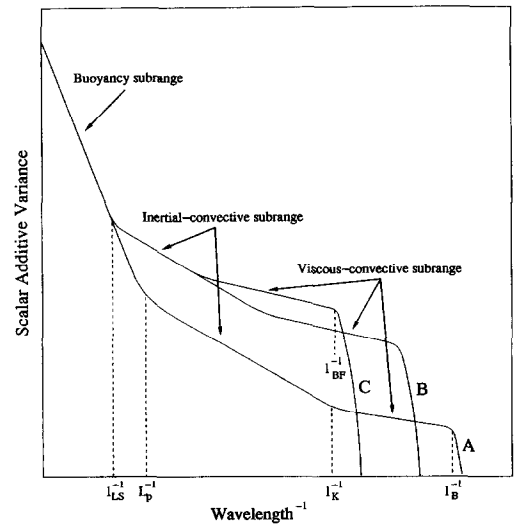

Fig. 3. A schematic of scalar fluctuation spectra versus inverse wavelength for progressive stages of turbulence fossilization. A: Active turbulence. B: Fossilization commences. C: Fossilization completed. See text for the definition of the variables.

How relevant is fossil turbulence to mesospheric radar scatter? Two possible effects come to mind. First, it can 'mask' the intermittent nature of the neutral turbulence in the radar backscatter data. That is, the radar will continue to detect electron density inhomogeneities even though the neutral turbulence may have dropped out momentarily. Completely fossilized electron density turbulence would present large reflectivities for a 50 MHz radar only if the electron Schmidt number is at least 100, because the cut-off length is $C_B l_{BF} \approx 3$ m for $Sc = 100$. ($Sc = 100$ in turn requires the presence of charged aerosols of size ~ 0.01 μm.)

Secondly, charged aerosols falling through a thin layer of turbulence will fossilize after descending to a region of calmness and will still create electron density inhomogeneities that scatter radar waves. However, the terminal velocity of an ice sphere of radius 0.01 μm is less than 0.1 m s^{-1}; thus, in 7 min the aerosol will fall no more than 40 m. Since this distance is well within the range resolution of all radars involved, this particular effect is not likely to be detected if it does occur.

The descent of fossil turbulence under gravity as described above may well account for the observations of mean downward Doppler velocities in the polar summer mesosphere. These were first reported by Balsley and Riddle (1984) and related to charged aerosols by Hall *et al.* (1992). However, the mechanism whereby the meter-scale structures were maintained during descent was not well developed in that paper and we suggest that the concept of fossil turbulence may be relevant.

3. ELECTRON DENSITY DEPLETION LAYERS

Electron density profiles often display bite-outs at the same height as simultaneously observed PMSE layers (Ulwick *et al.*, 1988; Inhester *et al.*, 1990; Röttger *et al.*, 1990). The best explanation we have so far for these thin depletion layers is the scavenging of electrons by aerosols (Pedersen *et al.*, 1970), specifically subvisible ice particles (Reid, 1990). The resultant sharp vertical gradients in the electron density at the top and bottom of the bite-outs may produce partial reflection of Fresnel scattering of the radar waves.

A sharp temperature minimum (or multiple minima) resulting from gravity wave modulation will force a correspondingly thin layer to be super-

saturated with respect to the water vapour. With the help of nucleation sites such as meteoric dust and water cluster ions, ice particles will form and grow within the cold layer. (Hall, 1990, has shown that gravity waves can also effectively modulate the formation of the cluster ions; thus, the density of nucleation sites may themselves be controlled by wave activity.) Free electrons will attach themselves to the ice, one or two electrons per aerosol on average (Jensen and Thomas, 1991). Since even very large ice cloud particles are expected to be charged with only four or five electrons, it is clear that only a large number of small ice particles will create a significant electron depletion (Reid, 1990). (A large number of large particles is not possible due to the limited amount of water vapour.) Therefore, noctilucent clouds are not expected to be co-located with electron density bite-outs. Furthermore, intense turbulence is not expected to coexist with the bite-outs since the consequent eddy diffusion would rapidly dissipate the depletion layer. Comparison of data from two rocket launches in which one exhibits turbulent plasma spectra and no electron bite-out, and the other shows non-turbulent spectra and a deep bite-out, supports this conclusion (Kelley and Ulwick, 1988). Both of these rocket flights occurred during strong PMSE.

Both partial reflection and Fresnel scattering require that the irregularities in the refractive index remain coherent in the horizontal direction over a Fresnel zone $f = (r\lambda_R/2)^{1/2}$, where r is the range and λ_R is the radar wavelength. For a 50 MHz radar, the horizontal correlation length must be greater than 500 m at 85 km. The manner in which the irregularities vary along the radar beam determines the difference between the two echoing mechanisms. Partial reflection is caused by long-lived vertical gradients, which can be described with deterministic functions. If the irregularities are randomly distributed within the radar volume, the echoing mechanism is called Fresnel scattering. Doviak and Zrnič (1984) and Balsley and Gage (1981) have studied the case where the correlation length is less than or equal to the Fresnel zone radius.

We can test the relevance of such Fresnel-type echoing mechanisms to PMSE by comparing the theoretical reflectivities calculated from rocket-derived refractive index profiles with the actual radar measurements. Woodman and Chu (1989) showed that the reflection coefficient depends very strongly on the shape, length scale, and smoothness of the refractive index profile. Therefore, we must be careful in choosing a function to interpolate between the discrete data points. The refractive index is the convolution of the data with an interpolation function. If this function has edges, extra reflection power is spuriously added because of the higher-order harmonics in these edges.

In the atmosphere, diffusion, possibly enhanced by turbulence, is the primary destruction mechanism of these irregularities. Since Green's function of the diffusion equation is a Gaussian, Woodman and Chu (1989) suggest using Gaussians to model the refractive index. We are currently working on such an approach. In order for this mechanism to be effective, the vertical length scale of the irregularities must be of the order of the radar Bragg wavelength (3 m for a 50 MHz radar). Such small structures could possibly be created because of the reduced electron diffusion caused by coupling to the charged aerosols. We note that Havnes *et al.* (1992) have proposed that the existence of neutral gas vortices in a field of falling charged aerosols would create 'forbidden zones' within the vortices, such that a very sharp density gradient would occur at the vortex walls. Partial reflection could then occur at the segment of the walls normal to the radar wave propagation.

4. DRESSED AEROSOLS

Picture an aerosol with charge number Z_a in a plasma. (Z_a can be positive or negative.) Statistically there will be a spherical 'cloud' of charge $-Z_a$ around the aerosol due to the average surplus or debit of free electrons. This shielding sphere will have a scale length given by the plasma Debye length

$$\lambda_D = \left(\sum_\alpha \frac{N_\alpha Z_\alpha^2 e^2}{\varepsilon_0 k T_\alpha} \right)^{-1/2} \tag{1}$$

where N is the number density, e is the charge of an electron, ε_0 is the free space permittivity, k is Boltzmann's constant, T is the temperature, and the subscript α refers to each of the plasma particle species.

Now send a radar wave through this 'dressed' aerosol. If $Z_a = 1$ then the scattered power will be exactly that of incoherent scatter. However, if the aerosol is multiply charged, and provided that the radar Bragg scale is much longer than the plasma Debye length, the electron 'cloud' around the aerosol will respond in phase to the wave and will thus increase the scattered amplitude by $|Z_a|$ and the power by Z_a^2. Since there was a decrease, by $|Z_a|$, in the number of free electrons involved, the per electron enhancement of scattered power over incoherent scatter is roughly proportional to $|Z_a|$.

The above scenario ignores the existence of other aerosols in the near vicinity. If another charged aerosol was placed closer to the original one than the plasma Debye shielding length, then their mutual

interaction will tend to cancel the enhancement. Therefore, two conditions need to be met for substantial enhancement of radar scatter over incoherent scatter to take place: (1) $\lambda_R/2 > 2\pi\lambda_D$ and (2) $N_a^{-1/3} \gg \lambda_D$.

This type of radio wave scattering was first proposed by Havnes *et al.* (1990) as an explanation for PMSE. We have also discussed it in an earlier paper (Cho *et al.*, 1992a) and showed that it can only be relevant for UHF PMSE. Here, we wish to discuss the second restriction, which we did not take into account previously.

If thermal equilibrium and a three-component plasma consisting of electrons, positive ions, and aerosols are assumed, (1) becomes

$$\lambda_D = 69\left(\frac{T}{N_e + N_i + Z_a^2 N_a}\right)^{1/2}. \quad (2)$$

With the charge neutrality condition $N_e = N_i + Z_a N_a$, (2) becomes

$$\lambda_D = 69\left[\frac{T}{2N_e + Z_a N_a (Z_a - 1)}\right]^{1/2}. \quad (3)$$

Comparing λ_D to the aerosol spacing $N_a^{-1/3}$ is not so straightforward since λ_D is a function of N_a. A useful alternative is to calculate the minimum aerosol charge required for a given aerosol abundance to fulfil $N_a^{-1/3} \gg \lambda_D$. In Fig. 4 the regions above the curves are

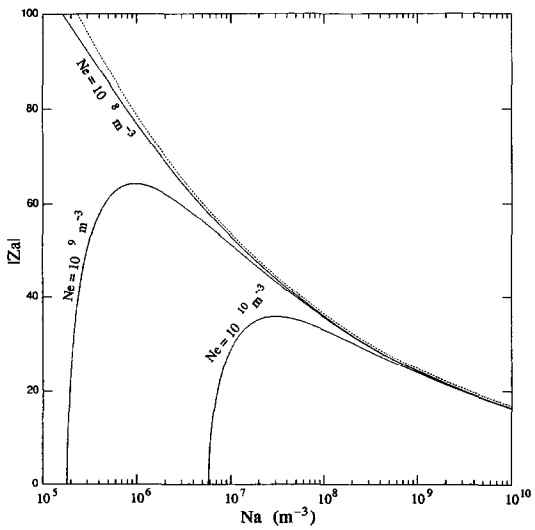

Fig. 4. Plots of minimum aerosol charge number required for dressed aerosol scatter versus aerosol number density. The regions above the curves for the different electron abundances are the regimes where the enhanced scattering can take place. The dotted line represents the case where only the aerosol Debye length is taken into account.

where significant signal enhancement over incoherent scatter can occur. We note that Hagfors (1992) uses λ_{Da}, the aerosol Debye length, instead of the plasma Debye length as the characteristic length scale of the dressed aerosol. This choice omits the dependency of the critical aerosol charge number on electrons and ions, and Fig. 4 correspondingly reduces to one curve, $|Z_a| = 69T^{1/2}N_a^{-1/6}$, wiping out an entire area of possible enhancement in the low-$|Z_a|$, low-N_a regime. This is a significant difference. We assert that the Debye length of the entire plasma mixture rather than just the aerosols must be considered since the fall-off of the aerosol electric potential depends on all the charged constituents. La Hoz (1992) is in agreement with our interpretation, but he does not make the point explicitly.

One can see that the most favourable condition for enhanced radar scatter is high electron density and low aerosol density. It is interesting to note that the two published reports of PMSE observed with UHF radars occurred after precipitation events, which increased the ambient electron density (Röttger *et al.*, 1990; Cho *et al.*, 1992a). Still, to produce the observed ~ 10 times enhancement in power above the incoherent scatter level, one needs at least $|Z_a| \sim 10$. Whether or not the mesopause aerosols are ever charged that highly is a big unknown at this point.

5. THE EFFECTS OF VERY SMALL, NEGATIVELY CHARGED AEROSOLS

The three-species plasma diffusion study of Cho *et al.* (1992a) showed that the presence of large charged aerosols reduces the electron diffusivity. However, Cho *et al.* (1992a) did not explicitly discuss the special case when the aerosols are very small and negatively charged. It turns out that there is a transition aerosol size, below which the electron diffusivity is actually enhanced. (Note, however, that positively charged aerosols will always reduce electron diffusivity.) In the limit of small aerosol size, such that it equals the size of the positive ions (i.e. the aerosols are negative ions), the electron diffusion equation reduces from the general coupled equations given by Cho *et al.* (1992a) to

$$\frac{\partial n_e}{\partial t} = 2D_i\left(1 + \frac{N_a}{N_e}\right)\nabla^2 n_e \quad (4)$$

where n_e is the electron density perturbation and D_i is the intrinsic ion diffusivity. Since the ambipolar diffusion coefficient for a two-species plasma (electron and positive ion) is $2D_i$, (4) implies that the electron diffusivity is enhanced by a factor of $(1 + N_a/N_e)$ when negative ions are introduced into the mixture. This

result agrees with the earlier work of Hill (1978). Numerical results from the general equations, allowing for different size negative particles, reveal that the transition from electron diffusion enhancement to reduction occurs when the aerosol radius is ~ 1 nm (Fig. 5).

This behaviour is not intuitively obvious, so let us try to form a qualitative picture. First, imagine a plasma mixture with just electrons and positive ions. If we introduce a perturbed area of high density for both species, the particles in the high density region will start to diffuse outward with the electrons tending to be on the outer edge due to their higher intrinsic diffusivity. Thus, the ambipolar electric field will be set up in such a way as to rein in the electrons and to tug the positive ions outward. Now introduce negative ions of size similar to the positive ones. (We maintain overall charge neutrality by subtracting electrons.) Because they are just as large as the positive ions, the negative ions will lag behind with the positive particles in the diffusion 'tug-of-war' with the electrons. Consequently, the ambipolar electric fields that the electrons experience will be 'watered down' by the addition of negative charge, and thus they will diffuse more rapidly. However, if we replace the negative ions with singly charged but very large negative aerosols, which diffuse even more slowly than the positive ions, then the 'tug-of-war' turns into a three-way competition with the negative aerosols holding back on the inside, the electrons pulling away on the outside, and the

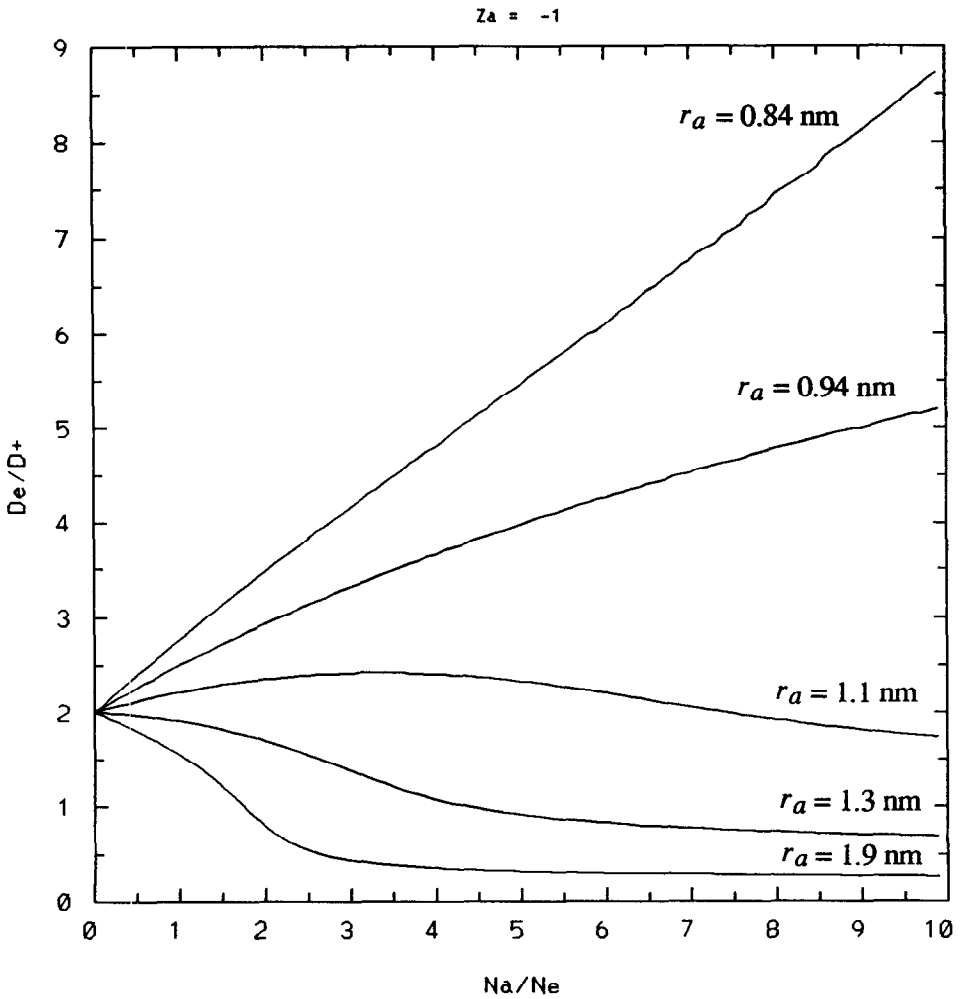

Fig. 5. Plot of effective electron diffusivity versus aerosol number density for positive ions with $Z_i = 1$ and negative ions or small aerosols with $Z_a = -1$. Electron diffusivity is normalized with respect to the positive ion diffusivity, and the aerosol number density is normalized with respect to the electron number density.

positive ions caught in between. Therefore, the reduction in the ambipolar field felt by the electrons will be counteracted by an overall decrease in the diffusivity due to the large negative aerosols. Thus, the transition from enhancement to reduction of effective electron diffusion occurs when the aerosol 'drag' starts to overcome the 'freeing up' effect of the diminished ambipolar electric field.

How does this diffusive transition phenomenon affect PMSE? Although negative ions are not believed to be prevalent in the summer mesopause region, negatively charged microclusters with radii less than 1 nm, thought to be meteoric smoke particles or newly nucleated ice aerosols, have been detected in the summer mesopause region (Schulte and Arnold, 1992). If such particles are numerous enough to dominate the plasma charge balance, then radar scattering will be actively suppressed due to the enhanced electron diffusivity.

As an aside to our discussion, the diffusive transition phenomenon is of interest in the interpretation of the D-region incoherent scatter radar spectral width, which is proportional to the effective electron diffusion coefficient. Equation (4) means that the presence of negative ions will broaden the spectral width. This conclusion agrees with the spectral width calculations of Mathews (1978) which has been used in the detection of negative ions with the Arecibo Observatory UHF radar (Ganguly *et al.*, 1979).

6. SEDIMENTATION EFFECTS

Statistically, the summer polar mesopause is at a height of 88 km (von Zahn and Meyer, 1989), while NLCs are observed at a mean of 83 km (Gadsden and Schröder, 1989). The altitude difference is caused by sedimentation. To illustrate this point, we show the growth and sublimation of a single ice particle using the model of Reid (1975) with a constant water vapour mixing ratio w and a temperature profile fitted to the mean given by von Zahn and Meyer (1989). Figure 6 shows the ice aerosol beginning its growth from a nucleation core of radius 0.3 nm at the mesopause, growing further as it falls, then quickly evaporating as the saturation ratio falls below unity with higher temperatures. The dashed curve is for a still atmosphere with $w = 1$ ppmv. A background velocity of 2 cm s^{-1} upward is assumed for the two solid curves, the left one with $w = 1$ ppmv and the right one with $w = 2$ ppmv. It is a simplified model in that the water mixing ratio is kept constant with time and that growth due to coagulation is neglected; however, it gives one an idea of what the aerosol size distribution with height may be like. It is not surprising then that

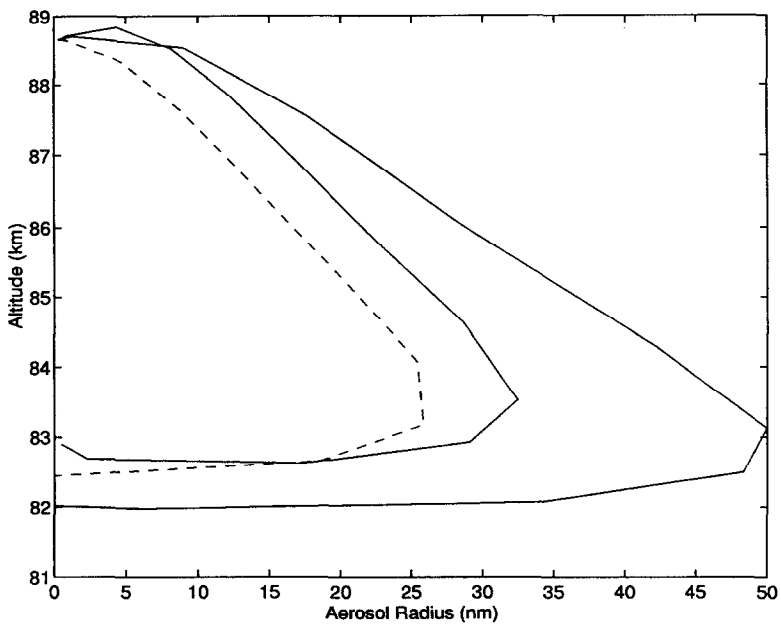

Fig. 6. Graph of the growth and evaporation of a falling ice sphere for (dashed) no background velocity with $w = 1$ ppmv, (solid, left) upward velocity of 2 cm s^{-1} with $w = 1$ ppmv, and (solid, right) upward velocity of 2 cm s^{-1} with $w = 2$ ppmv.

the average NLC (which requires particles of the order of 50 nm for visual detection) exists at 83 km, several kilometres below the mesopause. Logically, aerosols of intermediate size should occur between the two altitude limits.

The statistical peak of the PMSE profile is at 86 km, between the mesopause and NLC heights; this location can be explained in terms of the reduced diffusion theory as follows. There are two competing criteria for the enhancement of radar scatter by charged aerosols through reduced diffusion: (1) larger size and (2) dominance of overall plasma charge balance. Assuming a conservative limit on the charge per aerosol, and given the definite limit on the available water, the second criterion requires smaller (more numerous) particles. Thus, in light of the sedimentary size distribution over altitude, the maximum radar echo enhancement should, on the average, take place between the mesopause and NLC heights.

It also follows that the time lags associated with the nucleation, growth, sedimentation, evaporation, and water advection cycle of ice cloud formation affect the statistics of occurrence of PMSE and NLC. A model of this cycle by Sugiyama (1994) yielded out-of-phase oscillations between the cloud brightness and the nucleation layer. PMSE should then have a phase lag between the two. Perhaps it is not surprising that PMSE and ground-based NLC observations show no significant correlation in occurrence (Taylor *et al.*, 1989; Kirkwood *et al.*, 1994).

7. SUMMARY AND DISCUSSION

The summer mesopause region contains particles of disparate size, composition, and charge state: molecules, ions, electrons, dust and ice. We have seen that the coupling of electrons to the other species, especially charged ice aerosols, plays a crucial role in the production of PMSE.

In this paper, which is essentially a sequel to Cho *et al.* (1992a), we first investigated the phenomenon of fossil turbulence as applied to aerosols mixed by neutral gas turbulence. Because of their slow diffusivity, the aerosols can retain inhomogeneities in their distribution that appear spatially 'turbulent' even though the driving kinetic energy of the neutral gas turbulence has decayed. The electrons, following the pattern of the charged aerosols, will then also retain their density fluctuations which, in turn, will continue to scatter radar waves. The resulting radar Doppler spectra will be much narrower than those resulting from true turbulent scatter, a relevant point for PMSE since much of the observed Doppler spectra appear to be too narrow for turbulence-induced radar scatter.

Because the nucleation of ice particles is highly temperature dependent, they can form in thin layers within local temperature minima produced by gravity wave modulation. They can then grow and scavenge ambient electrons to create the oft-observed electron density depletion layers. The sharp variations at the edges of the electron density bite-outs may produce partial reflection or Fresnel scatter. The maintenance of such steep gradients is helped by the reduction of electron diffusivity due to the presence of the charged aerosols. Also, since the layers were produced by a particular gravity wave phase, they should be horizontally tilted parallel to the phase front. This mechanism could then account for the tilting of PMSE layers (van Eyken *et al.*, 1991).

When multiply charged, an aerosol will statistically 'dress' itself with a Debye sphere of surplus or debit of electrons, which respond in phase to the radar wave, thus leading to enhanced scatter above the level of classical incoherent scatter. For this dressed aerosol scatter to take place the radar wavelength must be much longer than the plasma Debye length and the spacing between aerosols must be longer than the plasma Debye length. We have considered more carefully the second restriction and have concluded that the most favourable condition for dressed aerosol scatter to take place in the mesosphere is high ambient electron density and low aerosol number density. It is intriguing that the two published cases of PMSE observed with UHF radars occurred during times of enhanced ambient electron density due to particle precipitation (Röttger *et al.*, 1990; Cho *et al.*, 1992b). However, the fundamental requirement that each aerosol be charged highly (more than ~ 10) is a difficult one to meet given the current understanding of the nature of the ice particles.

We then showed that negatively charged aerosols of radii less than 1 nm enhance electron diffusion, unlike positively charged aerosols and larger, negatively charged aerosols, which retard electron diffusion. If such particles are present and are numerous enough to dominate the overall plasma charge balance, then they will actually work to suppress radar scatter.

Consideration of sedimentation, along with the criterion that the aerosols could not be too small or too large, led us to conclude that the most effective enhancement of radar scatter due to reduced diffusion should occur between the mesopause and the average NLC height, a result that agrees with observations.

Finally, we pointed out that the time lags associated with ice cloud formation lead to a temporal phase difference between the formation of aerosols optimal for PMSE and the development of optically visible NLCs. Therefore, the observed non-correlation

between the occurrence of the two phenomena is not evidence against the charged aerosol theory of PMSE generation.

Acknowledgements—We would like to thank Don Farley and Tor Hagfors for helpful comments on dressed aerosol scatter. The Arecibo Observatory is part of the National Astronomy and Ionosphere Center, which is operated by Cornell University under a cooperative agreement with the National Science Foundation. The CUPRI was supported under NASA Grant NAG5-666, and NSF Grants ATM-9021915 and ATM-9217007. CMA was supported additionally by a NASA Graduate Student Research Program fellowship.

REFERENCES

Balsley B. B. and Gage K. S. 1981 On the vertical-incidence VHF backscattered power profile from the stratosphere. *Geophys. Res. Lett.*, **8,** 1173–1176.

Balsley B. B. and Riddle A. C. 1984 Monthly mean values of the mesospheric wind field over Poker Flat, Alaska. *J. Atmos. Sci.*, **41,** 2368–2375.

Batchelor G. K. 1959 Small-scale variation of convected quantities like temperature in a turbulent fluid, part 1. *J. Fluid Mech.* **5,** 113–133.

Cho J. Y. N. and Kelley, M. C. 1993 Polar mesosphere summer radar echoes: observations and current theories. *Rev. Geophys.* **31,** 243–265.

Cho J. Y. N., Hall T. M. and Kelley M. C. 1992a On the role of charged aerosols in polar mesosphere summer echoes. *J. Geophys. Res.* **97,** 875–886.

Cho J. Y. N., Kelley M. C. and Heinselman C. J. 1992b Enhancement of Thomson scatter by charged aerosols in the polar mesosphere: Measurements with a 1.29-GHz radar. *Geophys. Res. Lett.* **19,** 1097–1100.

Cho J. Y. N., Swartz W. E., Kelley M. C. and Miller C. A. 1993 CUPRI observations of PMSE during Salvo B of NLC-92: evidence of both partial reflection and turbulent scatter. *Geophys. Res. Lett.* **20,** 2291–2294.

Doviak R. J. and Zrnič D. S. 1984 Reflection and scatter formula for anisotropically turbulent air. *Radio Sci.* **19,** 325–336.

Ecklund, W. L., and Balsley B. B. 1981 Long-term observations of the Arctic mesosphere with the MST radar at Poker Flat, Alaska. *J. Geophys. Res.* **86,** 7775–7780.

Gadsden M. and Schröder W. 1989 *Noctilucent Clouds*. Springer-Verlag, Berlin.

Ganguly, S., Mathews J. D. and Tepley C. A. 1979 Thomson scatter radar detection of D-region negative ions at Arecibo. *Geophys. Res. Lett.* **6,** 89–92.

Gibson C. H. 1980 *Marine Turbulence*. Elsevier, Amsterdam, 221–257.

Gibson, C. H. 1982 On the scaling of vertical temperature gradient spectra. *J. Geophys. Res.* **87,** 8031–8038.

Gibson, C. H. 1986 Internal waves, fossil turbulence, and composite ocean microstructure spectra. *J. Fluid Mech.* **168,** 89–117.

Gibson C. H. 1991 Laboratory, numerical, and oceanic fossil turbulence in rotating and stratified flows. *J. Geophys. Res.* **96,** 12,549–12,566.

Hagfors T. 1992 Note on the scattering of electromagnetic waves from charged dust particles in a plasma. *J. Atmos. Terr. Phys.* **54,** 333–338.

Hall C. 1990 Modification of the energy-wavenumber spectrum for heavy proton hydrates as tracers for isotropic turbulence at the summer mesopause. *J. Geophys. Res.* **95,** 5549–5556.

Hall T. M., Cho J. Y. N., Kelley M. C. and Hocking W. K. 1992 A re-evaluation of the Stokes drift in the polar summer mesosphere. *J. Geophys. Res.* **97,** 887–897.

Havnes, O., de Angelis U., Bingham R., Goertz C. K., Morfill, G. E. and Tsytovich V. 1990 On the role of dust in the summer mesopause. *J. Atmos. Terr. Phys.* **52,** 637–643.

Havnes, O., Melandsø F., La Hoz C., Aslaksen T. K. and Hartquist T. 1992 Charged dust in the Earth's mesopause; effects on radar backscatter. *Phys. Scr.* **45,** 535–544.

Hill, R. J. 1978 Nonneutral and quasi-neutral diffusion of weakly ionized multiconstituent plasma. *J. Geophys. Res.* **83,** 989–998.

Hoppe U.-P., Hall C. and Röttger J. 1988 First observations of summer polar mesospheric backscatter with a 224-MHz radar. *Geophys. Res. Lett.* **15,** 28–31.

Inhester, B., Ulwick J. C., Cho J. Y. N., Kelley M. C. and Schmidt G. 1990 Consistency of rocket and radar electron density observations: Implication about the anisotropy of mesospheric turbulence. *J. Atmos. Terr. Phys.* **52,** 855–873.

Jensen E. J. and Thomas G. E. 1991 Charging of mesospheric particles: Implications for electron density and particle coagulation. *J. Geophys. Res.* **96,** 18,603–18,615.

Kelley, M. C. and Ulwick J. C. 1988 Large- and small-scale organization of electrons in the high-latitude mesosphere: Implications of the STATE data. *J. Geophys. Res.* **93,** 7001–7008.

Kelley M. C., Farley D. T. and Röttger J. 1987 The effect of cluster ions on anomalous VHF backscatter from the summer polar mesosphere. *Geophys. Res. Lett.* **14,** 1031–1034.

Kelley M. C., Ulwick J. C., Röttger J., Inhester B., Hall T. and Blix T. 1990 Intense turbulence in the polar mesosphere: Rocket and radar measurements. *J. Atmos. Terr. Phys.* **52,** 875–891.

Kirkwood S., Cho J. Y. N., Hall C. M., Hoppe U.-P., Murtagh D. P., Stegman J., Swartz W. E., van Eyken A. P., Wannberg G. and Witt G. 1995 A comparison of PMSE and other ground-based observations during the NLC-91 campaign. *J. Atmos. Terr. Phys.* **57,** 35–44.

Klostermeyer J. 1994 A two-ion ice particle model of the polar summer mesopause. *J. Geophys. Res.* **99,** 5487–5497.

Kolmogorov A. N. 1941 The local structure of turbulence in incompressible viscous fluids for very high Reynolds numbers. *Dokl. Akad. Nauk SSSR,* **30,** 301–305.

La Hoz C. 1992 Radar scattering from dusty plasmas. *Phys. Scr.* **45,** 529–534.

Lübken F.-J., Lehmacher G., Blix T. A., Hoppe U.-P., Thrane E. V., Cho J. Y. N. and Swartz W. E. 1993 First in-situ observations of neutral and plasma density fluctuations within a PMSE layer. *Geophys. Res. Lett.* **20,** 2311–2314.

Lumley, J. L. 1964 The spectrum of nearly inertial turbulence in a stably stratified fluid. *J. Atmos. Sci.* **21,** 99–102.

Mathews J. D. 1978 The effect of negative ions on collision-dominated Thomson scattering. *J. Geophys. Res.* **83,** 505–512.

Pedersen A., Tröim J. and Kane J. A. 1970 Rocket measurements showing removal of electrons above the mesopause in summer at high latitude. *Planet. Space Sci.* **18,** 945–946.

Reid, G. C. 1975 Ice clouds at the summer polar mesopause. *J. Atmos. Sci.* **32,** 523–535.

Reid G. C. 1990 Ice particles and electron 'bite-outs' at the summer polar mesopause. *J. Geophys. Res.* **95,** 13,891–13,896.

Röttger J., La Hoz C., Kelley M. C., Hoppe U.-P. and Hall C. 1988 The structure and dynamics of polar mesosphere summer echoes observed with the EISCAT 224-MHz radar. *Geophys. Res. Lett.* **15,** 1353–1356.

Röttger J., Rietveld M. T., La Hoz C., Hall T., Kelley M. C. and Swartz W. E. 1990 Polar mesosphere summer echoes observed with the EISCAT 933-MHz radar and the CUPRI 46.9-MHz radar, their similarity to 224-MHz radar echoes and their relation to turbulence and electron density profiles. *Radio Sci.* **25,** 671–687.

Schulte P. and Arnold F. 1992 Detection of upper atmospheric negatively charged microclusters by a rocket-borne mass spectrometer. *Geophys. Res. Lett.* **19,** 2297–2300.

Shur G. H. 1962 Experimental studies of the energy spectrum of atmospheric turbulence. *Proc. Central Aerolog. Obser. USSR* **43,** 79–90.

Stillinger D. C., Helland K. N. and Van Atta C. W. 1983 Experiments on the transition of homogeneous turbulence to internal waves in a stratified fluid. *J. Fluid Mech.* **131,** 91–122.

Sugiyama T. 1994 Ion-recombination nucleation and growth of ice particles in noctilucent clouds. *J. Geophys. Res.* **99,** 3915.

Taylor M. J., van Eyken A. P., Rishbeth H., Witt G., Witt N. and Clilverd M. A. 1989 Simultaneous observations of noctilucent clouds and polar mesospheric radar echoes: Evidence for non-correlation. *Planet. Space Sci.* **37,** 1013.

Ulwick J. C., Baker K. D., Kelley M. C., Balsley B. B. and Ecklund W. L. 1988 Comparison of simultaneous MST radar and electron density probe measurements during STATE. *J. Geophys. Res.* **93,** 6989–7000.

Ulwick J. C., Kelley M. C., Alcala C. M., Blix T. A. and Thrane E. V. 1993 Evidence for two different structuring and scattering mechanisms and the associated role of aerosols in the polar summer mesosphere. *Geophys. Res. Lett.* **20,** 2307–2310.

van Eyken A. P., Hall C. and Williams P. J. S. 1991 A determination of the orientation of Polar Mesosphere Summer Echo layers using the EISCAT as a dual beam radar, *Radio Sci.* **26,** 395–401.

von Zahn, U. and Meyer W. 1989 Mesopause temperatures in polar summer. *J. Geophys. Res.* **94,** 14,647–14,651.

Woodman R. F. and Chu Y. 1989 Aspect sensitivity measurements of VHF backscatter made with the Chung-Li radar: Plausible mechanisms. *Radio Sci.* **24,** 113–125.

Woods J. D. 1969 Fossil turbulence. *Radio Sci.* **4,** 1365–1367.